

MULTIPHASE EULERIAN SIMULATIONS OF A SEDIMENTATION PROCESS IN A SOLID-FLUID PARTICLE-LADEN FLOW

Csaba Klajbár¹, László Könözy²

*¹Ph.D. Student, Centre for Fluid Mechanics and Computational Science,
Cranfield University, Cranfield, Bedfordshire, MK43 0AL, United Kingdom*

*²Lecturer, Centre for Fluid Mechanics and Computational Science,
Cranfield University, Cranfield, Bedfordshire, MK43 0AL, United Kingdom*

ABSTRACT

In this paper, modelling details have been investigated for a multiphase settling process in a two-dimensional particle-laden flow. Unsteady simulations have been performed by using an Eulerian-Eulerian multiphase approach. A preliminary mesh sensitivity study showed that the numerical results might become oscillatory when the grid spacing is comparable with the solid particle diameter, which indicates that excessive mesh refinement is undesirable. In these multiphase flows, the interaction between the fluid and solid phases is modelled relying on purely heuristic arguments, which is a major source of uncertainties. Therefore fluid-solid exchange and drag coefficient models have been compared and assessed in terms of their accuracy. Since the ANSYS-FLUENT commercial software package provides only a few of these approaches, the majority of the models have been implemented through User-Defined Functions (UDFs) in C programming language. The results showed that the choice of an exchange model has considerable impact on the solution and the best agreement has been achieved by employing the formulation proposed by Schiller and Naumann [8]. However, only minor differences have been experienced between the distinct drag models for this specific problem due to their similar behaviour over the investigated settling Reynolds number range.

1. INTRODUCTION

The presence of additional phases in the primary continuum is common in industrial flows, so accurate predictions of multiphase flows is of interest in various computational fluid dynamics (CFD) applications. The currently investigated solid particle sedimentation in a liquid tank, which is also called as a fluid-solid interaction type problem, is not an exception. Batchelor [1] and Balakin et al. [2] published comprehensive investigations on the underlying physics of settling spherical particles in a sedimentation process with the integration to the Eulerian-Eulerian approach. In the work of Sobiesk [3], the importance of drag modelling is outlined for systems where spherical particles move in fluid flow. These authors highlighted that the computation of these systems also introduces uncertainties, because all parameters of the process such as the interaction between different phases are modelled relying on purely heuristic arguments. In the present work, we provide an overview on the Eulerian-Eulerian multiphase simulation capabilities for the aforementioned physical problem. Several interphase exchange models have been compared including the formulations of Gibilaro et al. [5], Gidaspow et al. [6], Huilin and Gidaspow [7], Schiller and Naumann [8], Syamlal and O'Brien [9], and

Wen and Yu [10]. Almost all of these models explicitly depend on the drag coefficient, therefore the drag models of Brown and Lawler [11], Cheng [12], Clift and Gauvin [13], Dalla Valle [14], Flemmer and Banks [15], Morsi and Alexander [16], and Orzechowski-Prywer [17] have been reviewed in the present paper.

1.1 PROBLEM FORMULATION

The sedimentation process in a two-dimensional multiphase solid-fluid particle laden flow has been investigated. A square-shaped tank with width of $x/H = 1.0$ and height of $y/H = 1.0$ has been considered, where H is the characteristic length. The initial homogeneous suspension of sand with volume fraction of $\alpha_s = 0.1$ is mixed with water from $y/H = 0.0$ to $y/H = 0.8$. The rest of the volume is filled with water (see Figure 1.1). The gravel with particle diameter of $d/H = 2 \cdot 10^{-3}$ settles to the bottom of the tank through gravitational acceleration. The water- and sand densities have been chosen as $\rho_w = 1000 \text{ kg/m}^3$ and $\rho_s = 2500 \text{ kg/m}^3$, respectively.

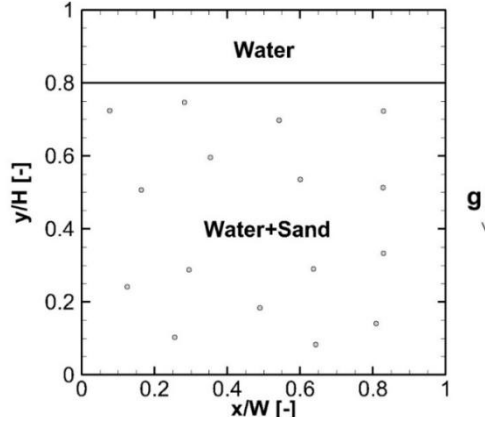


Figure 1.1: Initial sand suspension in the water tank ($t = 0$) [18].

2. GOVERNING EQUATIONS AND NUMERICAL METHODS

2.1 THE EULERIAN-EULERIAN MODEL

For modelling multiphase flows by employing the Eulerian-Eulerian approach, the phases are modelled as inter-penetrating and interacting continua on a shared computational domain. The momentum equation is solved for each phase and the interactions between different phases appear as additional source terms. The modified forms of the continuity and the momentum equations can be written as

$$\underbrace{\frac{\partial}{\partial t}(\alpha_q \rho_q)}_{\text{Mass rate of change}} + \underbrace{\nabla \cdot (\alpha_q \rho_q \mathbf{u}_q)}_{\text{Mass flux}} = \underbrace{\sum_{p=1}^2 (\dot{m}_{pq} - \dot{m}_{qp})}_{\text{Mass transfer rate}} + \underbrace{S_q}_{\text{Source}} = 0 \quad (2.1)$$

$$\begin{aligned}
\underbrace{\frac{\partial}{\partial t}(\alpha_q \rho_q \mathbf{u}_q)}_{\text{Mom. rate of change}} + \underbrace{\nabla \cdot (\alpha_q \rho_q \mathbf{u}_q \mathbf{u}_q)}_{\text{Momentum flux}} = & \underbrace{-\alpha_q \nabla p}_{\text{Pressure gradient}} + \underbrace{\nabla \cdot \mathbf{T}_q}_{\text{Strain tensor}} + \\
& + \underbrace{\alpha_q \rho_q \mathbf{g}}_{\text{Grav. force}} + \underbrace{\mathbf{R}}_{\text{Mom. exchange}} + \underbrace{\mathbf{S}_{F,q}}_{\text{Source}}
\end{aligned} \tag{2.2}$$

where the momentum exchange term can be expressed as

$$\mathbf{R} = \sum_{p=1}^2 \left(\underbrace{K_{sl}(\mathbf{u}_p - \mathbf{u}_q)}_{\text{Interphase mom. exchange}} + \underbrace{\dot{m}_{sl}\mathbf{u}_{sl} - \dot{m}_{ls}\mathbf{u}_{ls}}_{\text{Mom. rate of change}} \right) \tag{2.3}$$

The right-hand side of the continuity equation (2.1) is equal to zero, because there is no mass transfer rate taken into account for the investigated particle sedimentation case, thus the source term vanishes. The momentum equation (2.2) is solved with additional terms representing the momentum exchange (2.3) between the considered phases. It is important to mention that for modelling multiphase flows, these exchange terms cause the majority of uncertainties, because it includes parameters that are formulated relying on experiments and/or mathematical assumptions.

2.2 FLUID-SOLID EXCHANGE COEFFICIENTS

The momentum exchange term in Eq. (2.3) explicitly depends on the fluid-solid exchange coefficient K_{sl} , which has to be calibrated to take into account the momentum exchange between the phases. Therefore fluid-solid type models have been considered in the present work proposed by Gibilaro et al. [5], Gidaspow et al. [6], Huilin-Gidaspow [7], Schiller-Naumann [8], Syamlal-Obrien [9], and Wen-Yu [10]. The corresponding expressions for K_{sl} are summarized in Table 2.1.

Table 2.1: The investigated fluid-solid exchange models.

Exchange model	Expression
Gibilaro et al. [5]	$K_{sl} = \left(\frac{18}{Re_s} + 0.33 \right) \frac{\rho_l \alpha_s \mathbf{v}_s - \mathbf{v}_l }{d_s} \alpha_l^{-1.8}$
Gidaspow et al. [6]	$K_{sl} = \begin{cases} \frac{3\alpha_s \alpha_l \rho_l}{4d_s} \alpha_l^{-2.65} \mathbf{v}_s - \mathbf{v}_l c_D, & \text{if } \alpha_l > 0.8 \\ 150 \frac{\alpha_s (1-\alpha_l) \mu_l}{\alpha_l d_s^2} + 1.75 \frac{\rho_l \alpha_s \mathbf{v}_s - \mathbf{v}_l }{d_s}, & \text{if } \alpha_l \leq 0.8 \end{cases}$
Huilin-Gidaspow [7]	$K_{sl} = \psi \left(150 \frac{\alpha_s (1-\alpha_l) \mu_l}{\alpha_l d_s^2} + 1.75 \frac{\rho_l \alpha_s \mathbf{v}_s - \mathbf{v}_l }{d_s} \right) + (1 - \psi) K_{sl}^{W-Y}$
Schiller-Naumann [8]	$K_{sl} = \frac{3\alpha_s \mu_l Re_s}{4d_s^2} c_D$
Syamlal-Obrien [9]	$K_{sl} = \frac{3\alpha_s \alpha_l \rho_l}{4v_{r,s}^2 d_s} \left(\frac{Re_s}{v_{r,s}} \right) \mathbf{v}_s - \mathbf{v}_l c_D$
Wen-Yu [10]	$K_{sl} = \frac{3\alpha_s \alpha_l \rho_l}{4d_s} \alpha_l^{-2.65} \mathbf{v}_s - \mathbf{v}_l c_D$

2.3 DRAG COEFFICIENTS

It can be seen in Table 2.1 that the fluid-solid exchange coefficient formulations are functions of the drag coefficient (c_D), which is another critical point of an

accurate simulation for modelling the sedimentation process. The widely employed drag coefficient models have been summarized in Table 2.2. It is important to note that the drag coefficient can be written in different mathematical forms, all of them depend on the relative Reynolds number which can be expressed as

$$Re_s = \frac{\rho_s |\mathbf{v}_s - \mathbf{v}_l| d_s}{\mu_l} \quad (2.7)$$

where the velocity differences between the phases appear in the numerator. A preliminary analysis of the sedimentation problem showed that the maximal relative Reynolds number can be estimated as $Re_{s,max} = 4000$. In consequence of this, the drag coefficient functions have been shown in Figure 2.2 over the relative Reynolds number Re_s interval of interest. Note that all formulations show similar numerical behaviour up to $Re_s = 10$ except the Orzechowski-Prywer model [17]. When the dispersion is higher, deviations can also be expected at higher sedimentation rates.

Table 2.2: The investigated drag coefficient models.

Drag coefficient	Expression
Brown-Lawler [11]	$c_D = \frac{24}{Re_s} (1 + 0.15 Re_s^{0.681}) + \frac{0.407}{1 + 8710 Re_s^{-1}}$
Cheng [12]	$c_D = \frac{24}{Re_s} (1 + 0.27 Re_s)^{0.43} + 0.47 [1 - \exp(-0.04 Re_s^{0.38})]$
Clift-Gauvin [13]	$c_D = \frac{24}{Re_s} (1 + 0.15 Re_s^{0.687} + 0.0175 \frac{Re_s}{1 + 4.25 \cdot 10^4 Re_s^{-1.16}})$
Dalla Valle [14]	$c_D = (0.63 + 4.8 Re_s^{-0.5})^2$
Flemmer-Banks [15]	$c_D = \frac{24}{Re_s} 10^\alpha, \quad \alpha = 0.261 Re_s^{0.369} - 0.105 Re_s^{0.431} - \frac{0.124}{1 + \log^2 Re_s}$
Morsi-Alexander [16]	$c_D = a_1 + a_2 / Re_s + a_3 / Re_s^2$
Orzechowski-Prywer [17]	$c_D = \pi \left(0.128 + \frac{12.8}{Re_s} \right)$
Schiller-Naumann [8]	$c_D = \begin{cases} \frac{24}{Re_s} (1 + 0.15 Re_s^{0.687}), & \text{if } Re_s < 1000 \\ 0.44, & \text{if } Re_s \geq 1000 \end{cases}$

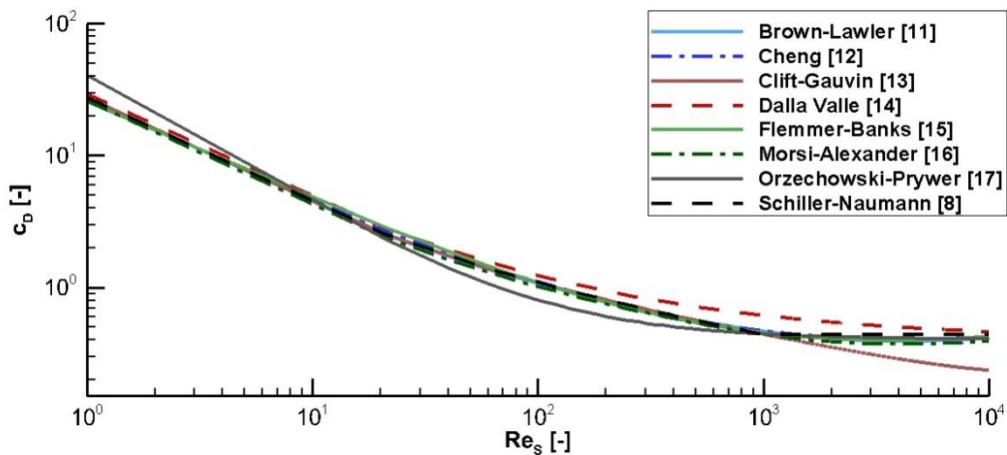


Figure 2.2: The drag coefficient models as function of relative Reynolds number.

2.4. NUMERICAL SIMULATION SETUP

Unsteady Eulerian-Eulerian simulations have been carried out by employing an implicit time-stepping algorithm. Uniform quadrilateral meshes have been used for a grid sensitivity study (see Figure 2.3). The most important mesh parameters have been summarized in Table 2.3. The time step size has been chosen for each grid individually in order to ensure appropriate temporal resolution and a constant Courant number of 0.365 has been kept relying on an estimated maximal settling velocity of $v_{s,max} = 0.3244 \text{ m/s}$. The computational domain boundaries have been treated as no-slip walls at $x/W = 0.0$, $x/W = 1.0$ and $y/H = 0.0$, and pressure outlet boundary condition has been prescribed for the edge at $y/H = 1.0$.

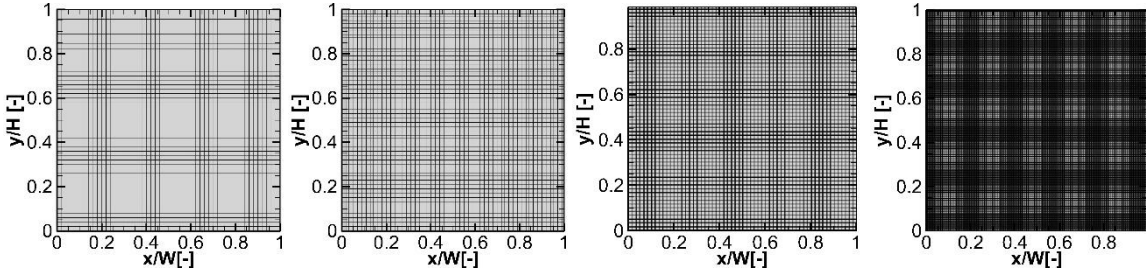


Figure 2.3: Computational grids used for a grid sensitivity study.

Table 2.3: Computational grid parameters.

Mesh	Coarse		Medium		Fine		Finer	
	N_x [-]	$\Delta x/d$ [-]	N_x [-]	$\Delta x/d$ [-]	N_x [-]	$\Delta x/d$ [-]	N_x [-]	$\Delta x/d$ [-]
Parameter	50	10.0	100	5.0	200	2.5	500	1.0

3. RESULTS AND DISCUSSION

The volume fraction distribution of the secondary phase (α_s) has been investigated at the $x/W = 0.5$ location along the y -coordinate direction at three dimensionless time levels ($t = 1, 2, 3$). Reference data were provided by Youngs [18] relying on the Eulerian/Lagrangian TURMOIL code. The overall model performances have been assessed by means of the L_0 and L_1 norms of the solid-phase volume fraction α_s as

$$||\alpha_s||_0 = \max |\alpha_{s,T} - \alpha_s|_{i=1,N} ||\alpha_s||_2 = \sqrt{\sum_{i=1}^N (\alpha_{s,T} - \alpha_s)^2} \quad (3.1)$$

where $\alpha_{s,T}$ denotes the reference TURMOIL values provided by Youngs [18].

3.1 RESULTS OF THE GRID SENSITIVITY STUDY

The results of the grid sensitivity study have been shown in Figure 3.1. By refining from the *Coarse* to *Fine* mesh, the accuracy of the solution is gradually improved. However, as the grid spacing becomes comparable with the particle diameter (*Finer* mesh), the solution becomes oscillatory. Balakin et al. [2] highlighted that this phenomenon is related to the modelling of granular flows, and the grid spacing has to be chosen appropriately to ensure the physical validity of the computations. Thus, the numerical investigations have been carried out by using the *Fine* configuration.

3.2 PREDICTION OF THE INTERPHASE EXCHANGE COEFFICIENT

Different interphase exchange-models, described above, have been employed in conjunction with drag coefficient models in terms of numerical accuracy. Figure 3.2 indicates obvious differences between various formulations. The model equations of Gibilaro et al. [5], Gidaspow et al. [6], Huilin-Gidaspow [7], Syamlal-Obrien [9] and Wen-Yu [10] produced significant discrepancy from the reference data [18] by predicting a lower sedimentation speed. In addition this, the theoretically maximal sand volume fraction of $\alpha_s = 1.0$ was considerably underestimated in certain cases (see Figure 3.2). The norms of the numerical results confirm these findings in a quantitative way (see Table 3.1). The best agreement was achieved by employing the Schiller-Naumann [8] model, therefore it was used for further computations.

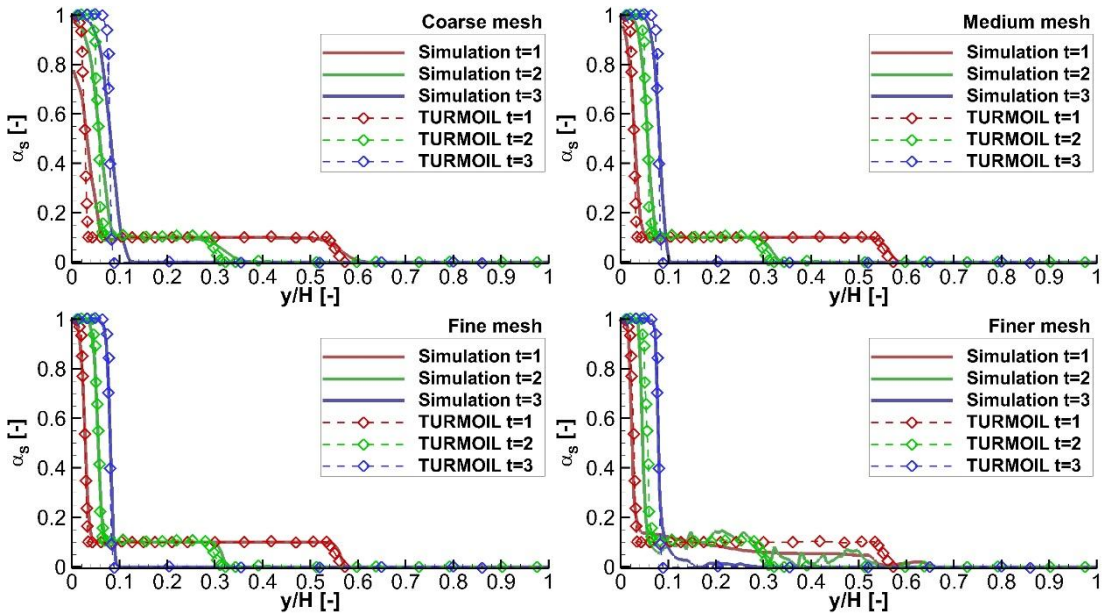


Figure 3.1: Predicted sand volume fraction distributions along the y -axis for four different computational meshes compared to the reference TURMOIL data [18] for the Schiller-Naumann model [8].

Table 3.2: L_0 and L_2 norms for the interphase exchange coefficient analysis.

Interphase Model	$t = 1s$		$t = 2s$		$t = 3s$	
	$\ \alpha_s\ _0$	$\ \alpha_s\ _2$	$\ \alpha_s\ _0$	$\ \alpha_s\ _2$	$\ \alpha_s\ _0$	$\ \alpha_s\ _2$
Gibilaro et al. [5]	0.2594	0.6089	0.2509	0.6538	0.5337	1.0156
Gidaspow et al. [6]	0.2892	0.5833	0.3948	0.8256	0.4524	0.7846
Huilin-Gidaspow [7]	0.2997	0.5992	0.4910	0.8797	0.4914	0.8416
Schiller-Naumann [8]	0.2475	0.4939	0.2026	0.4539	0.3484	0.6523
Syamlal-Obrien [9]	0.4466	0.9210	0.7064	1.5725	0.8230	1.5167
Wen-Yu [10]	0.2821	0.6033	0.3112	0.7040	0.3036	0.7500

3.3 DRAG MODEL ASSESSMENT

Drag coefficient models have been investigated by employing the Schiller-Naumann [8] exchange model due to its numerical accuracy for the sedimentation

problem presented in this paper (see Figure 3.2). The overall discrepancy between different models is lower than in the previous results (see Figure 3.3). This is due to the fact that the distinct functions results exhibit very similar characteristics in the investigated relative Reynolds number Re_s range. However, the qualitative measures indicate that the drag model of Brown and Lawler [11] slightly over-performed compared to the other models (see Table 3.3).

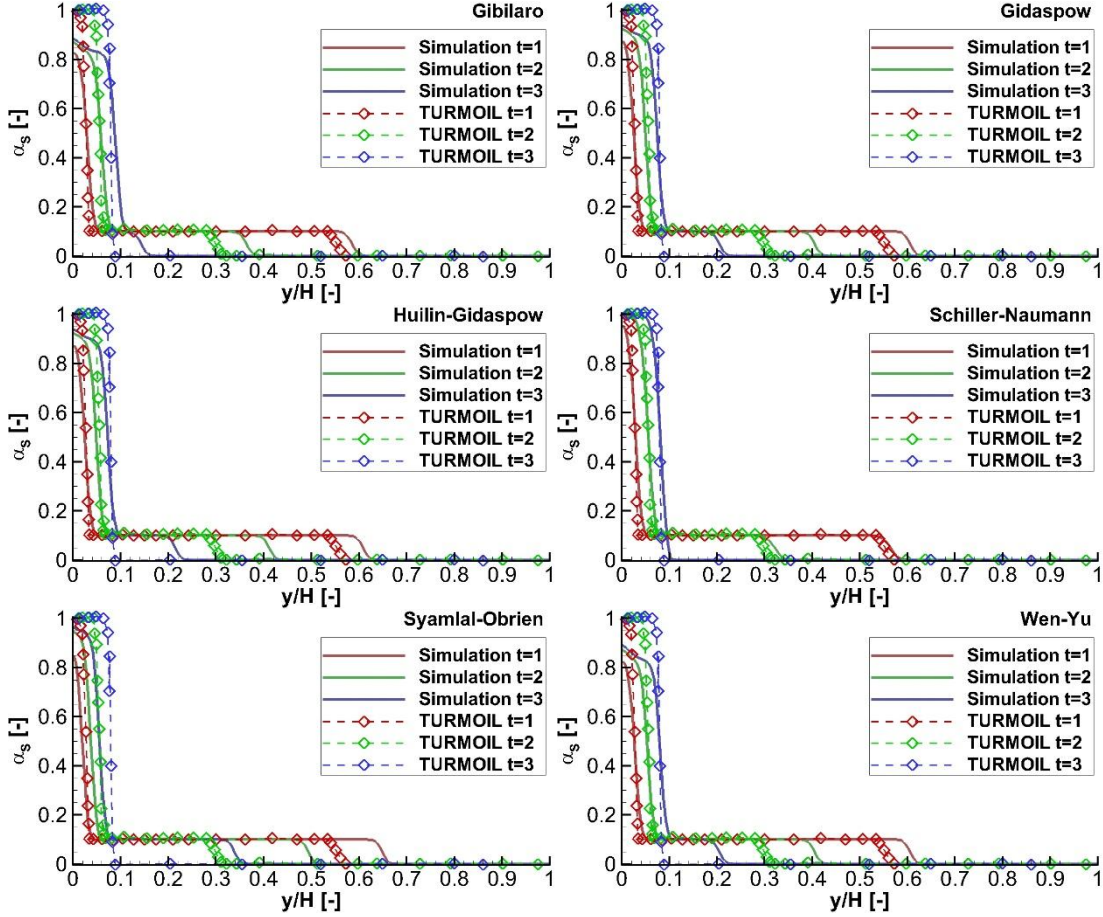


Figure 3.2: Predicted sand volume fraction distributions along the y -axis for various momentum exchange models compared to the reference TURMOIL data [18].

Table 3.3: L_0 and L_2 norms for the drag coefficient analysis.

Drag model	$t = 1s$		$t = 2s$		$t = 3s$	
	$\ \alpha_s\ _0$	$\ \alpha_s\ _2$	$\ \alpha_s\ _0$	$\ \alpha_s\ _2$	$\ \alpha_s\ _0$	$\ \alpha_s\ _2$
Brown-Lawler [11]	0.2439	0.4912	0.2101	0.4602	0.3460	0.6519
Cheng [12]	0.2481	0.4943	0.2009	0.4525	0.3485	0.6511
Clift-Gauvin [13]	0.2465	0.4932	0.2044	0.4554	0.3476	0.6511
Dalla Valle [14]	0.2588	0.5286	0.4063	0.8282	0.4957	0.8248
Flemmer-Banks [15]	0.2495	0.4960	0.1924	0.4447	0.3515	0.6150
Morsi-Alexander [16]	0.2551	0.5008	0.1922	0.4444	0.3421	0.6487
Orzechowski-Prywer [17]	0.3090	0.5859	0.2924	0.5443	0.3693	0.6862
Schiller-Naumann [8]	0.2475	0.4939	0.2026	0.4539	0.3484	0.6523

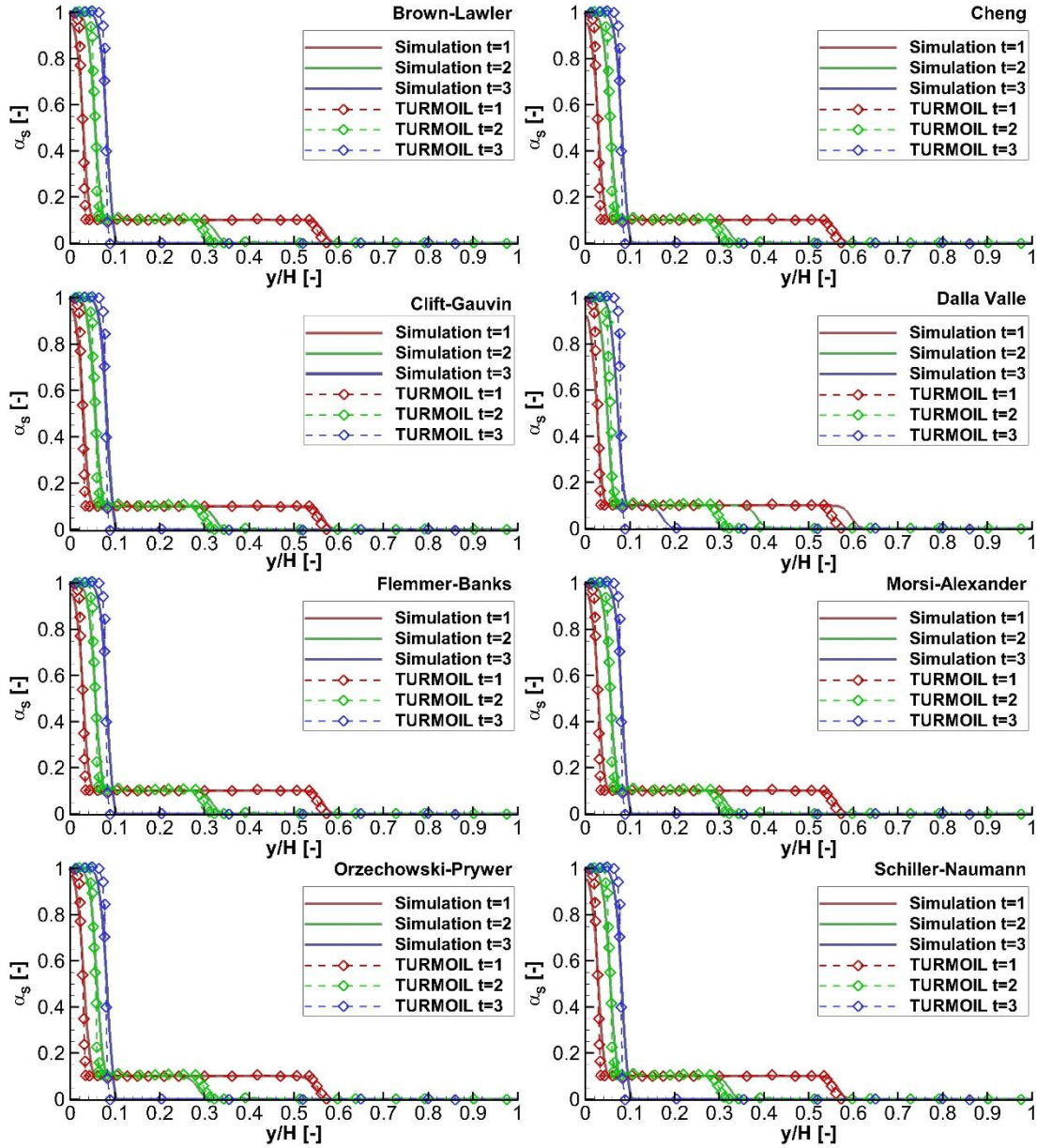


Figure 3.3: Predicted sand volume fraction distributions along the y -axis for various interphase exchange models compared to the reference TURMOIL data [18].

4. CONCLUSIONS

In this paper, an overview of possible tools is provided for simulating the settling process in a tank filled with mixture of water and sand particles. A comparative analysis have been carried out regarding grid spacing, interphase-exchange models and drag function models, and the results were compared to reference data in [18]. The analysis reflected that the grid refinement is effective up to a certain level, however excessively fine meshes produce instability in the numerical solution. It has also been shown that the choice of interphase-exchange model has strong impact on the solution accuracy. The model of Schiller-Naumann [8] was proven to be the most accurate for the presented sedimentation problem. The investigated drag function models produced small differences, because their behaviour is similar over

the relative Reynolds number of interest. The drag model of Brown-Lawler [11] produced the best agreement with reference data [18] in this particular case.

ACKNOWLEDGEMENT

The authors would like to acknowledge the reference data provided by Professor David Youngs in his lecture notes [18] at Cranfield University.

REFERENCES

- [1] Batchelor, G.K.: **Sedimentation in a Dilute Dispersion of Spheres**. J. Fluid Mech., 1982. Vol. 52(2), pp. 245-268.
- [2] Balakin, B.V., Hoffmann, A.C., Kosinski, P., Rhyne, L.D.: **Eulerian-Eulerian CFD Model for the Sedimentation of Spherical Particles in Suspension with High Particle Concentrations**. Eng. Appl. Comp. Fl. Mech., 2010. Vol. 4(1), pp. 116-126.
- [3] Sobieski, W.: **Drag Coefficient in Solid-Fluid System Modeling with the Eulerian Multiphase Model**. Drying Technol., 2011. Vol. 29, pp. 111-125.
- [4] ANSYS, Inc.: **ANSYS FLUENT Theory Guide**. ANSYS, Release 14.0, 2011.
- [5] Gibilaro, L.G., Di Felice, R., Waldram, S.P.: **Generalized Friction Factor and Drag Coefficient Correlations for Fluid-particle Interactions**. Chem. Eng. Sci., 1985. Vol. 40(10), pp. 1817-1823.
- [6] Gidaspow, D., Bezburuah, R., Ding, J.: **Hydrodynamics of Circulating Fluidized Beds, Kinetic Theory Approach**. In Fluidization VII, Proceedings of the 7th Engineering Foundation Conference on Fluidization, 1992. pp. 75-82.
- [7] Huilin, L., Gidaspow, D.: **Hydrodynamics of Binary Fluidization in a Riser: CFD Simulation Using Two Granular Temperatures**. Chem. Eng. Sci., 2003. Vol. 58, pp. 3777-3792.
- [8] Schiller, L., Naumann, Z.: **A Drag Coefficient Correlation**, Z. Ver. Deutsch. Ing., 77-318. 1935.
- [9] Syamlal, M., O'Brien, T.J.: **Computer Simulation of Bubbles in a Fluidized Bed**. AIChE Symp. Ser., 1989. Vol. 85, pp. 22-31.
- [10] Wen, C.Y., Yu, Y.H.: **Mechanics of Fluidization**. Chem. Eng. Prog. Symp. Ser., 1966. Vol. 62, pp. 100-111.
- [11] Brown, P.P., Lawler, D.F.: **Sphere Drag and Settling Velocity Revisited**. J. Environ. Eng., 2003. Vol. 129, pp. 222-231.
- [12] Cheng, N.S.: **Simplified Settling Velocity Formula for Sediment Particle**. ASCE J. Hydraul. Eng., 1997. Vol. 123, pp. 1491-1502.
- [13] Crowe, C.T., Schwarzkopf, D., Sommerfeld, M., Tsuji, Y.: **Multiphase Flows with Droplets and Particles**. CRC Press, Boca Raton. USA, 1998.
- [14] Dalla Valle, J.M.: **Micromeritics**. Pitman Pub. Corp., New York-London, 1948.
- [15] Flemmer, R.L.C., Banks, C.L.: **On the Drag Coefficient of a Sphere**. Powder Technol., 1986. Vol. 48(3), pp. 217-221.
- [16] Morsi, S.A., Alexander, A.J.: **An Investigation of Particle Trajectories in Two-Phase Flow Systems**. J. Fluid Mech., 1972. Vol. 55(2), pp. 193-208.
- [17] Panas, A.J., Faffinski, T.: **Comparative Analysis of Response of a Spherical Particle to One Dimensional Two-Phase Fluid Flow**. Eng. Model., 2008. Vol. 36, pp. 387-394.
- [18] Youngs, D.: **Application of the Lagrange-Remap Method to Compressible Multiphase Flows**. CFD for Multiphase Flows & Combustion, Lecture Notes, Cranfield University, Cranfield, Bedfordshire, United Kingdom, 2014. p. 90.